


# Technical Note: Patient dose from kilovoltage radiographs during motion-synchronized treatments on Radixact<sup>®</sup>

William S. Ferris<sup>a)</sup>  and Wesley S. Culberson 

Department of Medical Physics, School of Medicine and Public Health, University of Wisconsin-Madison, Madison, WI 53705, USA

(Received 9 June 2020; revised 27 August 2020; accepted for publication 27 August 2020; published 14 October 2020)

**Purpose:** Synchrony is a motion management system available on the Radixact linear accelerator that utilizes kilovoltage (kV) radiographs to track target motion and synchronize the delivery of radiation with the motion. Proper management of this imaging dose requires accurate quantification. The purpose of this work was to use Monte Carlo (MC) simulations to quantify organ-specific patient doses from these images for various patient anatomies.

**Methods:** Point doses in water were measured per TG-61 for three beam qualities commonly used on the Radixact. The point doses were used to benchmark a model of the imaging system built using the Monte Carlo N-Particle (MCNP) transport code. Patient computed tomography (CT) datasets were obtained for 5 patients and 100 planar images were simulated for each patient. Patient dose was calculated using energy deposition mesh tallies.

**Results:** The MCNP model was able to accurately reproduce the measured point doses, with a median dose difference of less than 1%. The median dose ( $D_{50\%}$ ) to soft tissue from 100 radiographs among the 5 patient cases ranged from 2.0 to 4.6 mGy. The max dose ( $D_{1\%}$ ) to soft tissue ranged from 6.2 to 31.0 mGy and the max dose to bony structures ranged from 20.2 to 71.7 mGy. These doses can be scaled to estimate total patient dose throughout many fractions.

**Conclusions:** Patient dose is largely dependent on imaging protocol, patient size, and treatment parameters such as fractionation and gantry period. Organ doses from 100 radiographs (an approximate number for one fraction) on the Radixact are slightly less than the doses from Tomo MVCT setup images. Careful selection of clinical protocols and planning parameters can be used to minimize risk from these images. © 2020 The Authors. *Medical Physics* published by Wiley Periodicals LLC on behalf of American Association of Physicists in Medicine. [<https://doi.org/10.1002/mp.14461>]

Key words: intrafraction imaging dose, Radixact, tomotherapy

## 1. INTRODUCTION

Active intrafraction motion management during radiotherapy often relies on kilovoltage (kV) imaging, magnetic resonance imaging (MRI), or radiofrequency tracking to determine the location of the target in real time.<sup>1</sup> Kilovoltage image tracking techniques deposit dose to the patient in addition to the dose from the therapy itself. The American Association of Physicists in Medicine (AAPM) Task Group 180 (TG-180) reported on management of imaging doses in radiation therapy, and recommends that imaging dose be considered in the treatment planning process if the dose will likely exceed 5% of the therapeutic dose.<sup>2</sup> Appropriate management of this imaging dose requires accurate quantification.

The Radixact linear accelerator (Accuray, Inc., Sunnyvale, CA) contains an optional motion management system called Synchrony<sup>®</sup>, which uses kV imaging during treatment to monitor the location of the target and synchronize the delivery of radiation with the motion of the target. A description of target tracking and motion of the jaws and multileaf collimator (MLC) during treatment has been provided in the works of Schnarr et al. and Chen et al.<sup>3,4</sup> Radiographs are acquired at two to six imaging angles every gantry rotation and are chosen by the operator. Synchrony can be used to manage both respiratory and nonrespiratory, or quasi-static

motion,<sup>3</sup> both of which require the use of kV radiographs during treatment.

Due to the recent release of Radixact Synchrony, there is limited literature on doses from kV radiographs acquired during these treatments. Accuray provides skin exposures at isocenter, which must be corrected for varying patient size and position and do not reflect dose at depth. Chen et al. measured the weighted computed tomography dose index ( $CTDI_w$ ) for 100 radiographs of the large thorax protocol on Radixact to be 8.4 mGy.<sup>4</sup> This value provides a magnitude of expected doses to water, but it does not consider patient anatomy, imaging protocol, or dose to materials other than water such as bone. The purpose of this work is to use measurements and simulations to quantify volumetric, organ-specific patient doses for various disease sites that may commonly be treated using Radixact Synchrony.

## 2. MATERIALS AND METHODS

A photograph of the kV imaging system mounted on the Radixact is shown in Fig. 1. The kV tube is manufactured by Siemens (Siemens AG, Munich, Germany) and is capable of tube potentials between 40 and 150 kVp. The kV tube is mounted 90° from the megavoltage (MV) source and is positioned such that the anode/cathode axis is parallel to the

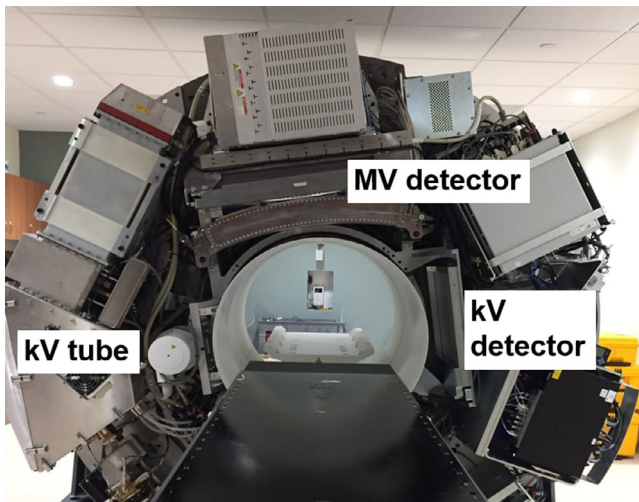


FIG. 1. Photograph of a Radixact at UW-Madison with the cover removed, showing the kV tube and flat panel kV detector. The MV source-to-axis distance (SAD) is 85 cm, the kV SAD is 57.5 cm, and the kV source to imager distance is 113.5 cm. The MV source is hidden in the picture by the couch. [Color figure can be viewed at wileyonlinelibrary.com]

direction of table travel. The beam is statically collimated to irradiate just inside the detector's usable pixels, which projects to approximately  $20 \times 20 \text{ cm}^2$  at isocenter. The beam qualities investigated in this work were 100, 120, and 140 kVp, which are the beam qualities used in the preset imaging protocols that come default on the Radixact, shown in Table I. The imaging protocol is the same for every angle used in the Synchrony treatment, that is, images at different angles cannot be set to different parameters.

## 2.A. Beam data measurements

The recommendations of the AAPM TG-61 were followed for measurement of kV point doses in water.<sup>5</sup> TG-61 specifies beam quality in terms of half-value layer (HVL), which were measured for each beam quality in millimeters of aluminum and millimeters of copper using an A12 ionization chamber (Standard Imaging, Middleton, WI). The filters were 99.9% pure and the thicknesses were specified to the nearest 0.001 mm. Narrow-beam geometry was obtained for the HVL measurements by addition of a lead diaphragm.

Point doses at depth in a water tank were determined using the TG-61 in-water method, described by Eq. (1).<sup>5</sup> The ion chamber was moved to each position at depth or off-axis with the water tank software and three measurements were acquired at each position. During each measurement, the couch and gantry were static, the kV imager was at zero degrees (pointing toward the floor), and the MV beam was off. The measured charge was fully corrected per TG-61 including a shutter correction. Air-kerma calibration coefficients were obtained for the A12 chamber from the University of Wisconsin Accredited Dosimetry Calibration Laboratory (ADCL) for medium-filtered beam qualities. The HVLs of the calibrated beam qualities bracketed the HVLs of the three Radixact beam qualities of interest and logarithmic

TABLE I. Default preset imaging protocols available for Synchrony treatments on Radixact.

Imaging protocol	mAs	kVp
XS thorax/pelvis	1	100
S thorax	0.8	120
S pelvis/ M thorax	1	120
M pelvis	1.25	120
L thorax	1.6	120
L pelvis	2	120
XL thorax/pelvis	4	140

interpolation was used to obtain the air-kerma calibration for each beam quality. The overall correction factor,  $P_{Q, \text{chamb}}$ , and the ratio of mean mass energy-absorption coefficient for water-to-air were obtained from the tables in TG-61 for the A12 chamber using the measured HVL of each beam. Field size correction factors were not used as these corrections are less than 1% for field sizes larger than the reference field size.<sup>5</sup> Point doses were acquired for one source-to-surface distance (SSD) for an inline profile, a crossline profile, and a depth-dose profile.

$$D_w = M \cdot N_k \cdot P_{Q, \text{chamb}} \cdot \left[ \left( \frac{\mu_{en}}{\rho} \right)_{\text{air}}^w \right]_{\text{water}} \quad (1)$$

## 2.B. Monte carlo modeling

The Monte Carlo N-Particle (MCNP) transport code version 6.2 was used for all simulations in this work.<sup>6</sup> The simulation geometry is shown in Fig. 2. A point source of photons was used for the starting particles for all simulations, which was set at depth in the anode to approximate the heel effect. The spectrum for each beam quality was obtained using the MATLAB code Spektr.<sup>7</sup> Beam hardening due to the inherent filtration, the mirror, and the monitor chamber were accounted for in the spectra of the starting particles using Spektr.

Energy deposition tallies were used for all tallies in this work. The tally results were converted to a dose in mGy/mAs using the following equation,

$$D_{MC} \left( \frac{\text{mGy}}{\text{mAs}} \right) = X_{MC} \left( \frac{\text{MeV}}{\text{g} \cdot \text{s.p.}} \right) \cdot \frac{D'_{Meas} \left( \frac{\text{mGy}}{\text{mAs}} \right)}{X'_{MC} \left( \frac{\text{MeV}}{\text{g} \cdot \text{s.p.}} \right)}, \quad (2)$$

where  $D'_{Meas}$  is the measured dose at the reference point in mGy/mAs,  $X'_{MC}$  is the simulated tally value at the reference point in MeV/g per source particle, and  $X_{MC}$  is the simulated tally value in the conditions of interest. Doses to water at the measurement points were calculated for the purpose of benchmarking the MCNP model.

## 2.C. Patient dose calculations

Five patient computed tomography (CT) datasets were acquired to be used for this imaging dose study. The disease

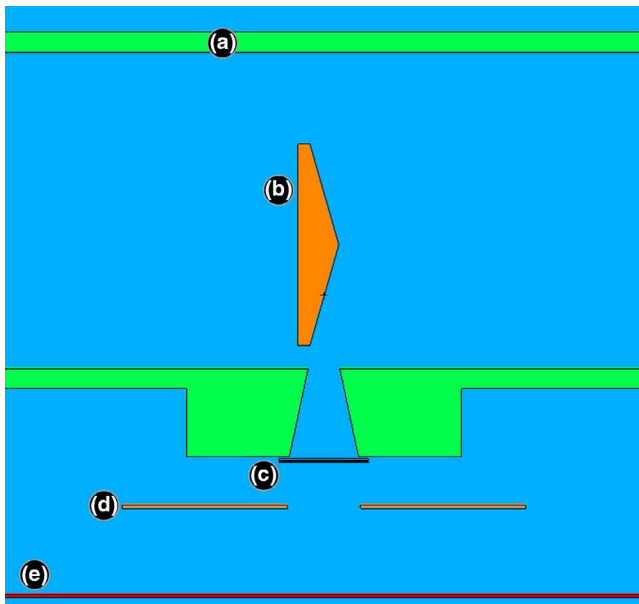


FIG. 2. Geometry of the MCNP simulations showing the kV tube shell (a), the tungsten anode (b), the 1 mm aluminum and 0.5 mm copper filters (c), the static tungsten collimator (d), and the 1.6 mm polycarbonate bore material (e). The anode–cathode axis is parallel to the direction of table travel. [Color figure can be viewed at [wileyonlinelibrary.com](http://wileyonlinelibrary.com)]

sites included in this work were lung (x2) and pancreas, which are likely candidates for respiratory Synchrony, and endothelium and prostate, which are likely candidates for nonrespiratory Synchrony motion management. All doses are provided for a single fraction and a standard number of radiographs per fraction (100). The imaging protocol for each patient was chosen based on patient size and disease site. The planning target volume (PTV) ranged from 2 to 146 cc among the five patients. Four or five imaging angles per gantry rotation were simulated in this work. Soft tissue was defined as all tissue excluding bone. The skin was defined as a 5 mm rind around the body. The CT datasets were aligned such that the target was centrally located in the bore (within the geometric restrictions of the bore). Couch travel was modeled by simulating the source at multiple superior/inferior locations for each gantry angle. The extent of superior/inferior point source locations was equal to the couch travel distance during treatment. The voxel size was  $2.5 \times 2.5 \text{ mm}^2$  or smaller in the axial plane and 3 mm or smaller in the superior/inferior direction. The carbon fiber couch of the Radixact was included in the simulations. Each voxel in the original CT image was assigned a physical density using a measured HU-to-density calibration phantom<sup>8</sup> and a material such as air, lung, adipose, muscle, cartilage, and bone based on the physical density. Equation (2) was used to convert the tally values into dose for each voxel. The dose calculation grid overlapped the CT grid.

### 3. RESULTS

The parameters used to determine point doses in water using the TG-61 protocol are shown in Table II. The standard

uncertainty ( $k = 1$ ) of the measured reference doses were estimated to be 4% based on the uncertainty of the measurements ( $<0.5\%$ ) and the 3.6% uncertainty reported in TG-61 for in-water point doses at the reference depth.<sup>5</sup> The standard uncertainty of nonreference-condition point doses (such as off-axis or depths not at 2 cm) was estimated to be 5%. The A12 ion chamber was observed to have a small energy dependence in the range of interest, as the air-kerma coefficients varied  $<0.2\%$  between tube potentials of 100 and 140 kVp.

Figure 3 shows a comparison of the measured and simulated point doses for each energy. The median and maximum global dose difference between the measured and simulated data were 0.6% and 6.0%, respectively.

Organ dose statistics are shown for each patient in Table III and example CT datasets and dose distributions for two of the patient cases are shown in Fig. 4. Doses are for 100 total images to approximate the number of images that may be delivered in one fraction. Simulation uncertainty in the MCNP 3D mesh dose was summarized for each patient case using the value  $u_{\text{med},10\%}$ , the median simulation uncertainty of voxels above 10% of the maximum dose. This value was 10% or less for all cases. The mesh doses are scaled by the reference dose measurements, whose uncertainty was estimated to be 4%. Therefore, the total uncertainty of voxel dose calculation in the patient geometries is estimated to have a median value of less than 11%, which is much less than the acceptable uncertainty of 20% stated in the TG-180 report.<sup>2</sup>

### 4. DISCUSSION

The MCNP model reproduced the measured point-dose data within a median difference of 0.8%. The asymmetric profile in the inline direction from the heel effect is reproduced (Fig. 3) by simulating the point source at depth in the anode, which allows for modeling changes in output and spectrum as a function of superior/inferior position. The accuracy of the model in reproducing the measured data was far better than the accuracy tolerance of  $\pm 20\%$  stated in TG-180 for imaging dose calculations during radiotherapy.<sup>2</sup>

The calculated doses to water in this work approximately agree with the work of Chen et al., who reported that the  $\text{CTDI}_w$  for 100 radiographs of the large thorax protocol (120 kVp, 1.6 mAs) was 8.4 mGy.<sup>4</sup> The point dose at isocenter for the large lung case using the large thorax imaging protocol in this work was 6.8 mGy. However, this work indicates

TABLE II. Parameters used for calculation of TG-61 point-doses in-water for three beam qualities commonly used on the Radixact.

Tube potential (kVp)	Measured HVL		$N_k$ (Gy/C)	$D'_{\text{Meas}}$ (mGy/mAs)
	(mm Cu, mm Al)			
100	0.50, 9.07		4.412E7	$0.120 \pm 0.005$
120	0.63, 10.17		4.408E7	$0.216 \pm 0.009$
140	0.77, 11.01		4.406E7	$0.336 \pm 0.013$

The conditions for the measured reference dose ( $D'_{\text{Meas}}$ ) were open field ( $20 \times 20 \text{ cm}^2$  at iso), 55 cm source-to-point distance (SPD), and 2 cm depth.

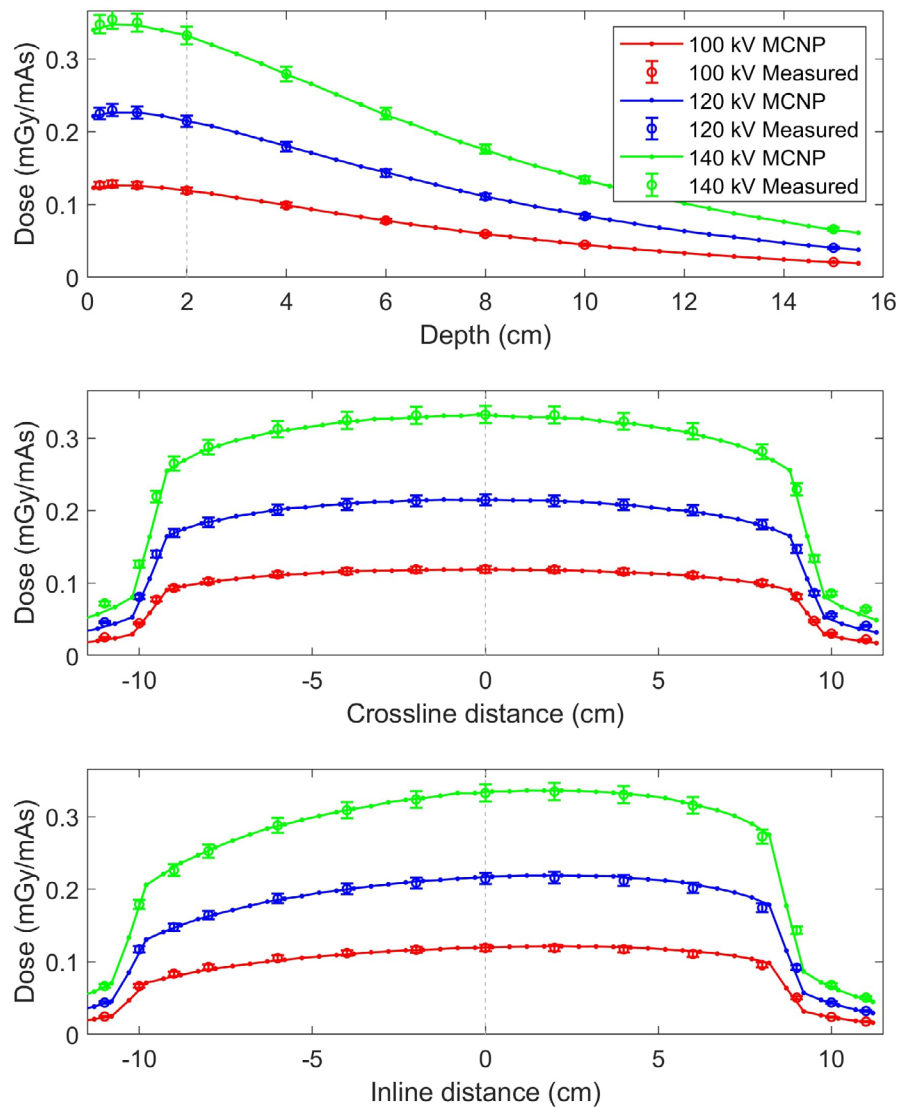


FIG. 3. Measured (A12) and simulated (MCNP) point-dose data in water for open-field radiographs ( $20 \times 20 \text{ cm}^2$ ). Error bars indicate standard error ( $k = 1$ ). The standard error of all simulated points was less than 0.5%. The heel effect can be observed in the inline direction via the asymmetric profile. The gray lines indicate the location of the reference point, at 2 cm depth and 55 cm from the source along the central axis. [Color figure can be viewed at [wileyonlinelibrary.com](http://wileyonlinelibrary.com)]

that doses to soft tissue may be much higher than  $\sim 7\text{--}8 \text{ mGy}$ , such as a max dose ( $D_{1\%}$ ) of 31.0 mGy for the endothelium patient imaged with the XL pelvis protocol. In addition, maximum doses to bony structures ranged from 20.2 to 71.7 mGy.

The data in this work suggest that patient dose is highly dependent on imaging protocol. The reference point dose was proportional to  $\text{kVp}^{3.1}$  when fit with the data in Table II. Dose at this point increases by a factor of 1.76 from 100 to 120 kVp and by a factor of 2.84 from 100 to 140 kVp. Patient dose also scales linearly with mAs, therefore patient dose can increase by a factor of 5 among the mAs protocol considered in this work. The values reported in this work can be scaled using the observed trends ( $\text{Dose} \propto \text{kVp}^{3.1} \cdot \text{mAs}$ ) to approximate doses when the clinical imaging protocol differs from the protocol used in this work.

Imaging protocol in this work was chosen based on the patient size and disease site alone. The imaging angles were

chosen to be approximately evenly spaced for this study. During a patient treatment, imaging protocol and angles can be chosen to optimize image quality and ensure visibility of the target. If angles are chosen such that they are unevenly spaced, this will result in a change in the hot and cold spots at the overlap of the beams. However, the user is prevented from choosing angles that are too close together and doses near the isocenter will likely not be largely changed since all imaging angles are centered on isocenter. The effect of varying imaging angles on patient dose was outside the scope of this work.

Patient anatomy and geometric setup also has a large effect on patient dose. The maximum dose ( $D_{1\%}$ ) to soft tissue ranged from 6.2 to 31.0 mGy among the five cases, which is a difference of a factor of 5. Even when scaled for kVp output using the fitted power law and to equal mAs, the maximum dose to soft tissue still varied by more than a factor of 2



TABLE III. Simulated patient dose in mGy from 100 radiographs.

Patient	$u_{\text{med},10\%T}$ (%)	$D_{\text{iso}}$	Volume	$D_{\text{ave}}$	$D_{50\%}$	$D_{10\%}$	$D_{1\%}$
Large lung <i>L thorax</i>	10	6.8	Heart	6.8	6.9	8.5	10.1
			Lungs	7.4	7.3	11.4	15.1
			Ribs	12.7	8.9	33.4	47.7
			Skin	3.8	1.5	11.4	16.3
			Soft tissue	4.6	3.5	10.1	15.0
Small lung <i>XS Thorax</i>	8	4.1	Heart	3.2	3.2	4.4	5.3
			Lungs	3.2	3.1	4.8	6.2
			Ribs	6.4	4.7	15.0	20.2
			Skin	1.7	1.1	4.2	6.6
			Soft tissue	2.2	2.0	4.4	6.2
Prostate <i>M Pelvis</i>	9	6.8	Spinal cord	6.6	6.4	10.0	32.2
			Bladder	7.2	6.9	9.2	10.7
			Pubic bone	11.9	12.6	19.1	26.0
			Prostate	5.4	5.4	6.1	6.8
			Rectum	6.0	6.1	7.3	8.2
Endothelium <i>XL Pelvis</i>	9	10.9	Skin	2.9	1.8	6.9	10.2
			Soft tissue	3.1	2.6	6.6	9.7
			Bladder	11.4	11.4	13.5	15.3
			Femurs	11.1	6.8	29.9	46.5
			Pubic bone	29.8	25.4	52.0	71.7
Pancreas <i>L Pelvis</i>	10	6.9	Rectum	12.8	12.6	16.5	20.5
			Skin	6.1	1.8	21.6	35.9
			Soft tissue	7.3	4.6	18.4	31.0
			Liver	8.3	8.3	10.6	13.3
			Lungs	4.4	3.7	8.4	11.9
			Pancreas	10.4	10.5	12.2	13.6
			Skin	3.9	1.5	11.7	18.2
			Soft tissue	4.5	3.0	10.6	15.5
			Spinal cord	5.9	5.9	9.7	16.7

Doses may be scaled to approximate dose from multiple fractions or varying number of total images. The imaging protocol used in the simulation is indicated in italics. The median simulation uncertainty of voxels above 10% of the maximum dose is denoted  $u_{\text{med},10\%T}$ .

among the five cases. The scaled maximum dose to soft tissue was lowest for the largest patients, since the individual fields are attenuated before overlapping. This can be observed in Fig. IV which displays dose distributions for a large and a small patient.

The attenuation of the couch used in this study was explored by simulating dose to a homogenous water phantom from a posterior to anterior beam with and without the couch. The average dose to a  $10 \times 10 \times 0.5 \text{ cm}^3$  volume on the surface of the water closest to the couch decreased by 5% and the dose to a point at 2 cm depth from the couch decreased by 8% when the couch was added. Therefore, skin entrance dose is expected to decrease by ~5% when imaging through the couch.

In addition to patient anatomy and imaging protocol, total patient dose will be highly dependent on treatment parameters. The number of images throughout a patient's treatment is a function of total treatment time and the number of active gantry rotations, since images are acquired every gantry rotation. Highly modulated treatments are more likely to have a tight pitch, leading to more gantry rotations per treatment and thus more total images. Treatments with a large number of fractions will likely have more total images since images must be acquired prior to starting the treatment to build the model of the target motion. In addition, the number of images per fraction might increase substantially if the treatment is paused regularly due to inaccurate target motion modeling, as new images must be acquired to resume the treatment each time the treatment is paused with the MV beam off.

Table IV compares the range of imaging doses in this work to imaging doses from other image-guidance procedures used in radiotherapy from the TG-180 report.<sup>2</sup> These data suggest that dose from 100 radiographs on the Radixact is expected to be slightly less than that from typical kV-CBCT scans or a Tomo MVCT setup scan.

Cumulative dose from kV images throughout many Synchrony fractions can be estimated by scaling the per fraction values provided in this work by the total number of images acquired throughout treatment. In an initial study with 13 Synchrony treatment plans with various fractionation schemes, the number of images per fraction ranged from 50 to 206, and the total number of images over all fractions ranged from 310 to 1920, with an average of 810 images.<sup>9</sup> When scaled to 2000 total images, the largest dose to any structure in Table III would be 1.4 Gy ( $D_{1\%}$  to the pubic bone for the endothelium patient). This value is slightly less than 5% of a typical therapeutic dose of 30, or 1.5 Gy. Therefore, it is expected that most cases will not exceed 5% of the therapeutic dose from these images alone, as 2000 images is an upper estimate and most therapeutic doses are greater than 30 Gy. However, these images will be combined with other routine imaging techniques and care should be used to reduce imaging dose from these procedures as choice of treatment parameters has a large effect on total number of images.

## 5. CONCLUSIONS

Monte Carlo simulations were used to calculate volumetric patient dose from 100 images on the Radixact with tube potentials between 100 and 140 kVp. Patient median doses to soft tissue and bony structures ranged from 2.0 to 4.6 mGy and 4.7 to 25.4 mGy, respectively. These doses are lower than that from other imaging procedures such as kV-CBCT or Tomo MVCT scans. Total patient dose will depend on imaging protocol, fractionation, and parameters such as number of gantry rotations, therefore careful planning can reduce imaging doses. The values in this work can be used by healthcare professionals to quantify patient imaging dose for typical treatment sites and manage risk from these procedures.

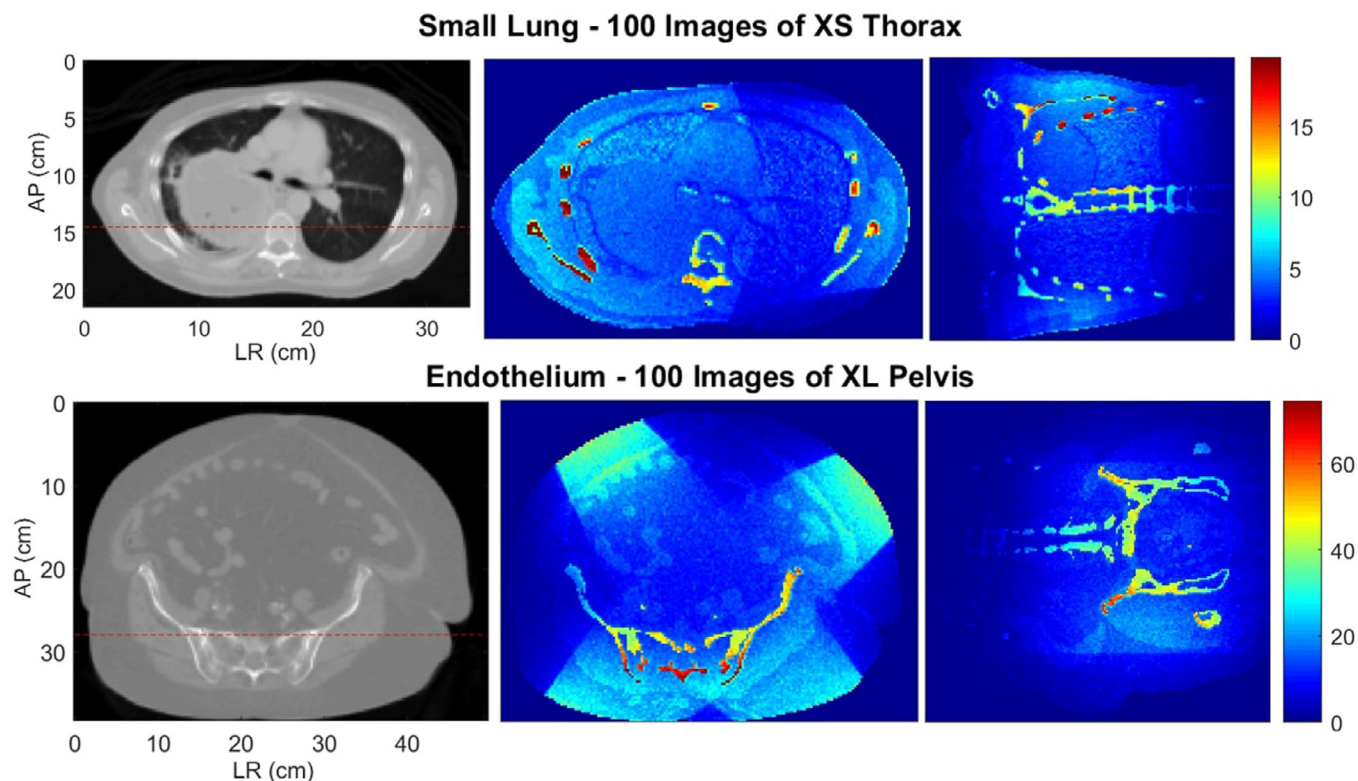


FIG. 4. Example computed tomography (CT) axial slices through isocenter and dose distributions in mGy resulting from 100 radiographs on the Radixact for two patient cases. Four imaging angles were used for the cases in this example. The target was placed at the geometric isocenter. The red line on the CT slice displays the AP location of the coronal dose distribution in this figure. Organ-specific dose statistics are provided for each patient case in Table III. [Color figure can be viewed at [wileyonlinelibrary.com](http://wileyonlinelibrary.com)]

TABLE IV. Comparison of imaging doses from 100 planar radiographs on the Radixact to doses from other imaging procedures.<sup>2</sup>

Procedure	Description	Dose range (mGy)
Radixact 100 radiographs	Soft tissue organs; median dose	1.6–12.6 <sup>a</sup>
Elekta pelvis kV-CBCT <sup>b</sup>	Soft tissue organs; median dose	9.0–20.0
Varian pelvis kV-CBCT	Soft tissue organs; median dose	11.9–19.9
Tomo MVCT setup scan	Isocenter of 30 cm water phantom	8.0–25.0 <sup>c</sup>

Analysis is limited to soft tissue organs and excludes the skin and the “soft tissue” contour.

<sup>a</sup>Range from five patient cases in this work.

<sup>b</sup>M cassette, no bow-tie filter, 120 kVp, 1 mAs/acquisition, 650 acquisitions.

<sup>c</sup>Range corresponds to the range of available pitches (coarse, normal, fine).

## ACKNOWLEDGMENTS

The authors thank the students and staff of the UWMRRC for their continued support, the UWRCL and UWADCL customers whose calibrations help support ongoing student research at the UWMRRC.

## CONFLICT OF INTEREST

The authors have no conflict of interest to disclose.

<sup>a</sup>Author to whom correspondence should be addressed. Electronic mail: [williamferris0@gmail.com](mailto:williamferris0@gmail.com); Telephone: (402) 889-3894.

## REFERENCES

- Keall PJ, Mageras GS, Balter JM, Emery RS, Forster KM, Jiang SB. The management of respiratory motion in radiation oncology report of AAPM Task Group 76. *Med Phys.* 2006;33:3874–3900.
- Ding GX, Alaei P, Curran B, et al. Image guidance doses delivered during radiotherapy: quantification, management, and reduction: report of the AAPM therapy physics committee task group 180. *Med Phys.* 2018;45:e84–e99.
- Schnarr E, Beneke M, Casey D, et al. Feasibility of real-time motion management with helical tomotherapy. *Med Phys.* 2018;45:1329–1337.
- Chen GP, Tai A, Keiper TD, Lim S, Li XA. Technical note: comprehensive performance tests of the first clinical real-time motion tracking and compensation system using MLC and jaws. *Med Phys.* 2020;47:2814–2825.
- Ma CM, Coffey CW, DeWerd LA, et al. AAPM protocol for 40–300 kV x-ray beam dosimetry in radiotherapy and radiobiology. *Med Phys.* 2001;28:868–893.

6. Werner CJ. MCNP6.2 Release Notes. Los Alamos National Laboratory report LA-UR-18-20808; 2018.
7. Siewerdsen JH, Waese AM, Moseley DJ, Richard S, Jaffray DA. Spektr: a computational tool for x-ray spectral analysis and imaging system optimization. *Med Phys*. 2004;31:3057–3067.
8. Constantinou C, Harrington JC, DeWerd LA. An electron density calibration phantom for CT-based treatment planning computers. *Med Phys*. 1992;19:325–327.
9. Ferris WS, Kissick MW, Bayouth JE, Culberson WS, Smilowitz JB. Evaluation of radixact motion synchrony for 3D respiratory motion: modeling accuracy and dosimetric fidelity. *J Appl Clin Med Phys*. 2020;21:96–106. <https://doi.org/10.1002/acm2.12978>.